Chapter 3

Two-dimensional nonlinear time fractional reaction–diffusion equation in application to sub-diffusion process of the multicomponent fluid in porous media

3.1 Introduction

In this chapter, a two-dimensional mathematical model describing diffusion of solute in porous media is considered. A significant portion of fractional calculus theory is the two-dimensional fractional differential equations and integral equations which have further been studied in the articles [74, 75, 76, 77, 78]. In [79], the authors have solved the two-dimensional fractional percolation equation in a non-homogeneous porous medium. In the present chapter, an accurate and efficient numerical technique has been proposed to solve two-dimensional fractional order reaction-diffusion equation arising in porous media.

Several kinds of flow problems like percolation flow problems, seepage flow problems have been examined and discussed in many aspects of research fields including groundwater hydraulics, seepage hydraulics, fluid dynamics and groundwater dynamics arising in the

porous media [80, 81]. The two-dimensional flow of the solute in the porous medium is governed under the hypothesis of continuity and Darcy's law is given by Bear and Verruijt [13] in the equation

$$\frac{\partial}{\partial x}(k_x \frac{\partial P}{\partial x}) + \frac{\partial}{\partial y}(k_y \frac{\partial P}{\partial y}) = A_0 \frac{\partial P}{\partial t}, \quad (x, y) \in \Omega, \tag{3.1}$$

where A_0 denotes the specific storativity, which is approximated by the effective porosity or specific yield; P denotes the pressure head, the intrinsic permeability of the medium is given by $K = \frac{k\rho g}{\mu}$, which is the hydraulic conductivity having the components in the x, y directions as k_x and k_y; ρ denotes the water density ; μ be the viscosity; and g the gravitational acceleration; Ω is the percolation domain.

Since there is a large digression from the ordinary Gaussian diffusion, therefore the underlying superposition is not appropriate in tracing the movement of the solute concentration in a porous medium which is non-homogeneous. Additionally, a supplementary realistic model can be obtained by the consideration of the application of fractional order density gradient to recapture the non-homogeneity of the porous medium. The Modified Darcy law was proposed by the authors of [82] with Riemann-Liouville fractional order derivative. Under the assumption of the continuity of seepage flow and the Darcy law, the percolation equation (3.1) is deduced into the the following forms as these assumptions are not valid for real seepage flow. The differential system with ordinary derivative does not quantify the flow of fluid with spatial path dependency and/or time memory. This limitation in the application of ordinary differential system has motivated the authors of [82] to model the fractional Darcy law.

$$q_x = k_x \frac{\partial^{\alpha_1} P}{\partial x^{\alpha_1}}, \quad 0 < \alpha_1 < 1, \tag{3.2}$$

and

$$q_y = k_y \frac{\partial^{\alpha_2} P}{\partial y^{\alpha_2}}, \quad 0 < \alpha_2 < 1. \tag{3.3}$$

In the special case, the usual Darcy law can be obtained by putting $\alpha_1 = \alpha_2 = 1$.

The variations of the solute concentration with respect to the column length and time depend upon the several species and factors in fluid. It is very hard to find the overshoots of probability density function for the several cases like conservative and non-conservative systems. In addition to this, interactions of the solutes with medium or other species play a significant role in the flow of the fluid through porous media. In order to analyze the diffusion of the solute in porous media in two-dimension, an attempt has taken in the present chapter to develop a two-dimensional sub-diffusion physical model with the prescribed initial and boundary conditions given below, where the fractional derivative is

taken in Caputo sense. The fractional time derivative corresponds to long-time heavy tail decay.

$$\frac{\partial^\alpha u}{\partial t^\alpha} = \frac{\partial}{\partial x}(u\frac{\partial u}{\partial x}) + \frac{\partial}{\partial y}(u\frac{\partial u}{\partial y}) + ku(1-u);\ 0 < \alpha < 1, \\ 0 \le x \le 1, 0 \le y \le 1, \tag{3.4}$$

with initial and boundary conditions as

$$\begin{aligned} u(x,y,0) &= 0, \\ u(0,y,t) &= c_0, \\ u_x(1,y,t) &= 0, \\ u_y(x,0,t) &= 0, \\ u_y(x,1,t) &= 0, \end{aligned} \tag{3.5}$$

where α is an arbitrary fractional order, k denotes the reaction coefficient and c_0 be a constant. For the approximation of solute concentration Kronecker product is used which is discussed later.

3.2 The General Conservation Principle

In this section of the chapter, a fluid continuum in flowing state is considered. In general a multi-component fluid has been considered in such a way that it follows the continuum approach and each component in itself is a continuum filling of the entire space, as in Fig. 3.1. Let H_a be the initial amount of the the extensive fluid property (e.g., mass) is contained in a volume V within a portion of space at time t and enclosed by a surface S. Consider the position of the system at time $t + \triangle t$, in the time interval $\triangle t$, the system moves and gets deformed. At time t, the system is of surface area S and volume V, whereas the system at time $t + \triangle t$ is of volume V' and surface S'. These are composed of the regions: $V = V_1 + V_2, V' = V_2 + V_3$. The region V_2 is common to V and V'.

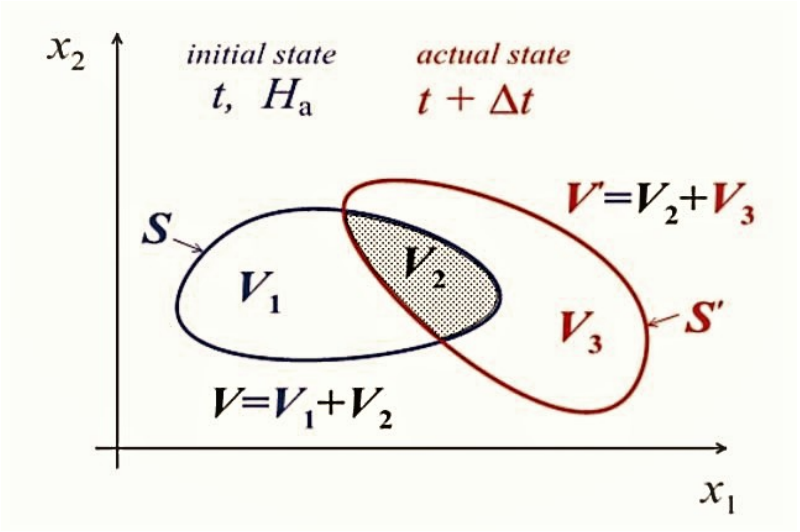

FIGURE 3.1: Fluid continuum in the flowing process

In Lagrange point of view, the temporal rate of change $(D/Dt)H_a$ of H_a for the moving system is given by

$$\frac{DH_a}{Dt}|_{system} = \lim_{\triangle t\to\infty}\{\frac{[(H_a)_2+(H_a)_3]_{t+\triangle t}-[(H_a)_1+(H_a)_2]_t}{\triangle t}\}, \tag{3.6}$$

where

$$(H_a)_i = \int_{(V_i)} \rho_a\gamma_a dV = \int_{(V_i)} h_a dV,\ \ i=1,2,3; H_a/\delta V = h_a. \tag{3.7}$$

The general conservation principle of a property for the species $'a'$ is given by

$$\partial h_a/\partial t + \mathrm{div}(h_a V_{H_a}) = I_a, \tag{3.8}$$

where I_a is the temporal rate per unit volume and V_{H_a} is the velocity field.

3.2.1 Mass conservation of species

Mass conservation of the fluid across a porous material involves the fundamental principle that total mass flux entered minus total mass flux out equals to the increase in mass amount stored by the medium. This means that the total mass of fluid is conserved. For a system of multi-component fluid of a species $'a'$, substituting $h_a = \rho_a$ and $V_{H_a} = V_a$ in the above equation, we get

$$\partial\rho_a/\partial t + \mathrm{div}(\rho_a V_a) = I_a, \tag{3.9}$$

where I_a is the rate at which mass of the species $'a'$ produced per unit volume during the chemical reaction in the system. From the Eulerian point of view, above equation is the equation of continuity (or equation of mass conservation) [83].

If we assume the case of stationary fluid and $I_a = 0$ then from above, the Fick's second law is deduced for diffusion for binary fluid as

$$\partial \rho_a / \partial t = \text{div}(D_{ab} \text{grad} \rho_a), \tag{3.10}$$

where D_{ab} is the diffusion coefficient.

3.3 Kronecker Product and its some properties

In this section some basic and fundamental properties of the well known Kronecker product are defined [84, 85]. Furthermore, we try to give some overview of the applications and properties of the Kronecker Product, which is an operation between two arbitrary size matrices represented by the symbol $\otimes$.

Definition 1. The Kronecker product of the matrix A of order $p \times q$ and B of order $m \times n$ is again $pm \times qn$ order block matrix, which is denoted by $A \otimes B$ and is defined by

$$A \otimes B = \begin{bmatrix} a_{11}B & a_{12}B & \dots & a_{1q}B \\ a_{21}B & a_{22}B & \dots & a_{21}B \\ \vdots & \vdots & \vdots & \vdots \\ a_{p1}B & a_{p2}B & \dots & a_{pq}B \end{bmatrix}. \tag{3.11}$$

Moreover, If A and B represent some linear transformations on vector spaces i.e., $W_1 \to V_1$ and $W_2 \to V_2$, respectively, then $A \otimes B$ represents the tensor product of these two maps, $W_1 \otimes W_2 \to V_1 \otimes V_2$.

3.3.1 Basic Properties of Kronecker Product

Since Kronecker product is a special case of tensor product, therefore it can satisfy the property like associativity and bi-linearity. Also, it has a lot of interesting and effective properties, few are stated below as

$$I \otimes (J + K) = I \otimes J + I \otimes K, \tag{3.12}$$

$$(I + J) \otimes K = I \otimes K + J \otimes K, \tag{3.13}$$

$$(kI \otimes J) = (I \otimes kJ) = k(I \otimes J), \tag{3.14}$$

$$(I \otimes J) \otimes K = I \otimes (J \otimes K), \tag{3.15}$$

where I, J and K are arbitrary matrices and k is a scalar.

3.4 Laguerre operational matrix for fractional order differentiation

The definition of Laguerre polynomials and its some properties are discussed in section (2.3) of Chapter 2. In similar manner to the equation (2.16) and (2.18) of Chapter 2, an arbitrary two-dimensional function $u(x, y, t) \in L^2[0, 1]$ can be approximated in terms of Laguerre polynomial as

$$u(x, y, t) \simeq u_N(x, y, t) = \sum_{g=0}^{N} \sum_{h=0}^{N} \sum_{i=0}^{N} b_{g,h,i} \Omega_g(x) L_h(y) L_i(t) = \sigma(t)^T \cdot B \cdot \sigma(x) \otimes \sigma(y), \tag{3.16}$$

where the unknown constant matrix $B = [b_{g,h,i}]$ is the Laguerre coefficient. These coefficients can be determined by using the initial and boundary conditions.

The operational matrix for fractional differentiation of order α is derived in the Theorem 2.2. This operational matrix can be written in the following form.

$$ {}_0^C D_t^\alpha \sigma(t) = H^{(\alpha)} \sigma(t), \tag{3.17}$$

where H^α is an operational matrix with fractional derivatives of $N + 1 \times N + 1$ order and is given as

$$H^{(\alpha)} = \begin{bmatrix} 0 & 0 & 0 & \dots & 0 \\ \vdots & \vdots & \vdots & \cdots & \vdots \\ 0 & 0 & 0 & \cdots & 0 \\ P_\alpha(\lceil\alpha\rceil, 0) & P_\alpha(\lceil\alpha\rceil, 1) & P_\alpha(\lceil\alpha\rceil, 2) & \cdots & P_\alpha(\lceil\alpha\rceil, N) \\ \vdots & \vdots & \vdots & \cdots & \vdots \\ P_\alpha(i, 0) & P_\alpha(i, 1) & P_\alpha(i, 2) & \cdots & P_\alpha(i, N) \\ \vdots & \vdots & \vdots & \cdots & \vdots \\ P_\alpha(N, 0) & P_\alpha(N, 1) & P_\alpha(N, 2) & \cdots & P_\alpha(N, N) \end{bmatrix}. \tag{3.18}$$

3.5 Implementation of Laguerre operational matrix

Here we are going to apply the fractional operational matrix on concerned two-dimensional mathematical model using Laguerre collocation method.

Now, in view of the equation (3.16), we shall approximate the solute concentration $u(x, y, t)$ in the form of Laguerre polynomials in the following manner as

$$u(x,y,t) = \sum_{f=0}^{N}\sum_{g=0}^{N}\sum_{h=0}^{N} c_{fgh} L_f(x) L_g(y) L_h(t), \tag{3.19}$$

where c_{ghi} is the Laguerre coefficients, where $g = 1, 2, 3, \cdots; h = 1, 2, 3, \cdots; i = 1, 2, 3, \cdots;$ The equation (3.19) can be represented in vector form as

$$u(x,y,t) = \sigma(t)^T \cdot B \cdot \sigma(x) \otimes \sigma(y), \tag{3.20}$$

where $B = [c_{fgh}]$ is a matrix of order $(N+1) \times (N+1)^2$ of constant Laguerre coefficients and $\sigma(t) = [L_0(t), L_1(t), \cdots, L_r(t)]^T$ is a column vector.

Applying the fractional derivative of order α with respect to time variable t on equation (3.20) and using the equation (3.17), we get

$$\frac{\partial^\alpha u}{\partial t^\alpha} = H^\alpha u(x,y,t) = [H^\alpha \cdot \sigma^T(t)] \cdot B \cdot \sigma(x) \otimes \sigma(y). \tag{3.21}$$

Similarly,

$$\frac{\partial u}{\partial x} = Hu(x,y,t) = \sigma^T(t) \cdot B \cdot (H^1 \times I) \cdot \sigma(x) \otimes \sigma(y), \tag{3.22}$$

$$\frac{\partial u}{\partial y} = Hu(x,y,t) = \sigma^T(t) \cdot B \cdot (I \times H^1) \cdot \sigma(x) \otimes \sigma(y). \tag{3.23}$$

In above equations I be the $(N+1) \times (N+1)$ identity matrix. Now from prescribed initial and boundary conditions (3.5) with the aid of equation (3.20), we get

$$\begin{aligned}
&\sigma^T(0) \cdot B \cdot \sigma(x) \otimes \sigma(y) = 0,\\
&\sigma^T(t) \cdot B \cdot \sigma(0) \otimes \sigma(y) = c_0,\\
&\sigma^T(t) \cdot B \cdot (H^1 \times I) \cdot \sigma(1) \otimes \sigma(y) = 0,\\
&\sigma^T(t) \cdot B \cdot (I \times H^1) \cdot \sigma(x) \otimes \sigma(0) = 0,\\
&\sigma^T(t) \cdot B \cdot (I \times H^1) \cdot \sigma(x) \otimes \sigma(1) = 0.
\end{aligned} \tag{3.24}$$

Now, we collocate equation (3.4) with the help of equations (3.24) at points $x_b=\frac{b}{N}$ for $b = 0, 1, 2, \cdots, N$, $y_b=\frac{b}{N}$ for $b = 0, 1, 2, \cdots, N$ and $t_b=\frac{b}{N}$ for $b = 0, 1, 2, \cdots, N$. Using these collocation points and fractional operational matrix, a nonlinear system of algebraic equations is found. On simplifying this system, we can calculate the Laguerre coefficients matrix B which can further be used in equation (3.20) to find the approximate numerical solution.

3.6 Error bound of the approximation

In this section the upper bound of the error of proposed numerical approximation is estimated by using Theorem 2.3 and equation (2.42) of Chapter 2.

Theorem 3.1. *Suppose $u(x, y, t)$ be the sufficiently smooth function on the region A and $(\frac{\partial^\alpha u}{\partial t^\alpha})_N$ be the approximation of $(\frac{\partial^\alpha u}{\partial t^\alpha})$. Then the approximated error $(\frac{\partial^\alpha u}{\partial t^\alpha})$ by $(\frac{\partial^\alpha u}{\partial t^\alpha})_N$ is bounded by*

$$| E(N) | \leq \sum_{f=0}^{N}\sum_{g=0}^{N}\sum_{h=0}^{N} \frac{c_{fgh}}{f!\cdot g!\cdot m!}\cdot \chi_{mhN}\cdot e^{\frac{x+y+t}{2}}, \quad x, y, t \geq 0, \quad f, g, m = 0, 1, 2, \cdots; \tag{3.25}$$

where $\chi_{mbN} = \sum_{m=0}^{N} S_\alpha(b, m)$.

Proof. In view of the equation (3.19), we have

$$u(x, y, t) = \sum_{f=0}^{N}\sum_{g=0}^{N}\sum_{h=0}^{N} c_{fgh}L_f(x)L_g(y)L_h(t), \tag{3.26}$$

truncating it upto $N + 1$ terms, we have

$$u_N(x, y, t) = \sum_{f=0}^{N}\sum_{g=0}^{N}\sum_{h=0}^{N} c_{fgh}L_f(x)L_g(y)L_h(t). \tag{3.27}$$

We can write α order partial derivative of $u(x, y, t)$ and $u_N(x, y, t)$ w.r.to t as

$$\frac{\partial^\alpha u}{\partial t^\alpha} = \sum_{f=0}^{N}\sum_{g=0}^{N}\sum_{h=0}^{N} c_{fgh}L_f(x)L_g(y)\frac{\partial^\alpha L_h(t)}{\partial t^\alpha}, \tag{3.28}$$

$$(\frac{\partial^\alpha u}{\partial t^\alpha})_N = \sum_{f=0}^{N}\sum_{g=0}^{N}\sum_{h=0}^{N} c_{fgh}L_f(x)L_g(y)\frac{\partial^\alpha L_h(t)}{\partial t^\alpha}. \tag{3.29}$$

From the above equations, we can write

$$E(N) = \frac{\partial^\alpha u}{\partial t^\alpha} - (\frac{\partial^\alpha u}{\partial t^\alpha})_N = \sum_{f=0}^{N}\sum_{g=0}^{N}\sum_{h=0}^{N} c_{fgh} L_f(x) L_g(y) \frac{\partial^\alpha L_h(t)}{\partial t^\alpha}. \tag{3.30}$$

Using equation (2.30) of Chapter 2, the above equation reduces to

$$\mid E(N) \mid = \mid \sum_{f=0}^{N}\sum_{g=0}^{N}\sum_{h=0}^{N} c_{fgh} L_f(x) L_g(y) (\sum_{m=0}^{N} S_\alpha(b,m) L_m(t)) \mid, \tag{3.31}$$

or,

$$\mid E(N) \mid = \sum_{f=0}^{N}\sum_{g=0}^{N}\sum_{h=0}^{N} c_{fgh} L_g(y) \cdot \chi_{mhN} \mid L_f(x) \mid \cdot \mid L_g(y) \mid \cdot \mid L_m(t) \mid . \tag{3.32}$$

Applying equation (2.42), we get

$$\mid E(N) \mid \leq \sum_{f=0}^{N}\sum_{g=0}^{N}\sum_{h=0}^{N} c_{fgh} \cdot \chi_{mhN} \cdot \frac{1}{m!} e^{\frac{t}{2}} \cdot \frac{1}{f!} e^{\frac{x}{2}} \cdot \frac{1}{g!} e^{\frac{y}{2}}. \tag{3.33}$$

Using the formulae S1 and S2 given in [86] and subtracting the truncated series from the infinite series, bounding each term in the difference, and summing the bounds complete the proof of the theorem. □

3.7 Numerical simulations and error analysis

Laguerre fractional operational matrix has been applied on some existing fractional order problems to find their approximate numerical solutions. The obtained numerical results have been compared with the existing analytical solutions through finding the absolute error for approximation to illustrate the capability and validity of the proposed numerical scheme. All the numerical calculations are carried out by using the software MATHEMATICA 11.3.

The absolute error is defined by [87] as

$$E_{abs}(x,y,t) = \mid u_{exact} - u_{num}(x,y,t) \mid . \tag{3.34}$$

Maximum error for the problem in x for fixed y and t is defined as

$$\mathrm{Max}E_{abs}(x, 0.5, 0.5) = \max_{0\leq x\leq 1} \mid E_{abs}(x, 0.5, 0.5) \mid . \tag{3.35}$$

The absolute error for the concerned test examples with a fix value of t and x is given by

$$\mathrm{Max}E_{abs}(0.5, y, 0.5) = \max_{0\leq y\leq 1} \mid E_{abs}(0.5, y, 0.5) \mid . \tag{3.36}$$

The order of convergence for two successive approximations $N_1$and N_2 is also calculated to validate the higher order accuracy of the numerical scheme which is given as

$$Order = \frac{\log(\frac{\mathrm{Max}E_{abs}(N_1)}{\mathrm{Max}E_{abs}(N_2)})}{\log(\frac{N_2}{N_1})}, \tag{3.37}$$

where $\mathrm{Max}E_{abs}(N)$ is the maximum absolute error during the approximation of degree N.

Example 1. Let us consider a two-dimensional non-linear non-homogeneous fractional order advection-diffusion equation as

$$\frac{\partial^\alpha u}{\partial t^\alpha} = \frac{\partial^2 u}{\partial x^2} + \frac{\partial^2 u}{\partial y^2} + \frac{\partial u}{\partial x} + \frac{\partial u}{\partial y} + \frac{u^2}{3} + f(x, y, t), \tag{3.38}$$

with $f(x, y, t) = -x\sqrt{t} - y\sqrt{t} - \frac{x^2y^2t}{3} - \frac{0.682734xy}{t^{0.3}}$ under the given initial and boundary conditions as

$$\begin{aligned} &u(x, y, 0) = 0, \\ &u(0, y, t) = 0, \\ &u(x, 0, t) = 0, \\ &u(1, y, t) = y\sqrt{t}, \\ &u(x, 1, t) = x\sqrt{t}. \end{aligned} \tag{3.39}$$

For the above example, the exact solution is $u(x, y, t) = xy\sqrt{t}$ for the fractional order parameters $\alpha = 0.8$. The absolute errors between the results obtained by our proposed numerical scheme and the exact solutions are exhibited through Table 3.1 and Table 3.2 for $y = 0.5, 0 \leq x \leq 1$ and $x = 0.5, 0 \leq y \leq 1$, respectively for the order of approximation $N = 5, 7, 9$ at $t = 1$. The tables clearly confirm that the order of convergence for the proposed method increases as the degree of Laguerre polynomials in x and y increases. Again absolute error decreases with the increase of the order of approximation of the polynomial

N, which clearly shows the effectiveness of the proposed numerical scheme. Again the data of CPU time shows that it takes minimum time to obtain accurate result showing that the method is computationally effective to solve the two-dimensional fractional order PDEs.

TABLE 3.1: Efficiency of the numerical method for Example 1 at $y = t = 0.5$

y	N	Maximal absolute error $0 \leq x \leq 1$	Order of convergence	CPU TIME (second)
0.5	5	0.00063	-	7.22
	7	0.000098	5.53	8.48
	9	0.000008	9.96	12.39

TABLE 3.2: Efficiency of the numerical method for Example 1 at $x = t = 0.5$

x	N	Maximal absolute error $0 \leq y \leq 1$	Order of convergence	CPU Time (second)
0.5	5	0.00071	-	7.21
	7	0.000084	6.27	8.48
	9	0.0000071	9.92	12.39

The absolute error is graphycally shown through Fig. 3.2 for various values of y and t for a fixed value of $x = 0.5$. Fig. 3.2 shows that the numerical solution is approximately accurate to the exact solution even for small value $N = 5$, the better convergence can be achieved increasing N. Thus comparing the numerical solution with the exact solution, we can say that the proposed method is very much efficient.

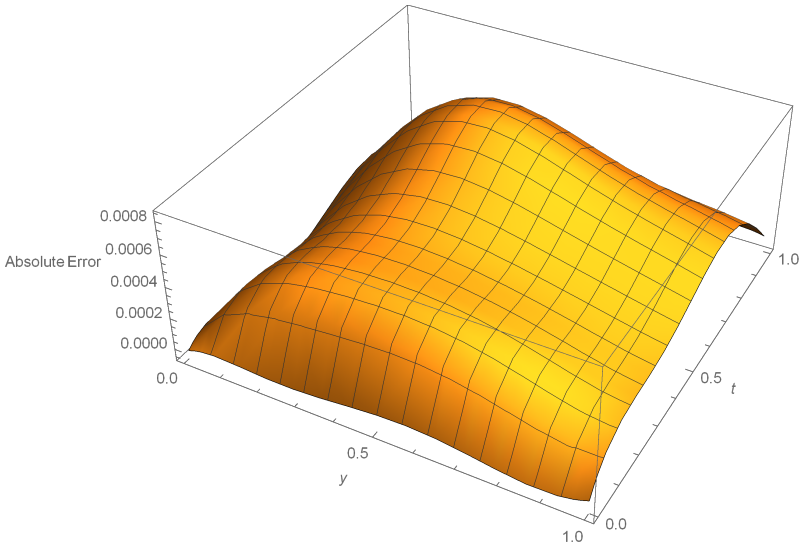

FIGURE 3.2: Plot of the absolute error between the exact and numerical solutions vs. y and t at $x = 0.5$

Example 2. Consider time-fractional non-linear Fisher's equation as

$$\frac{\partial^\alpha u}{\partial t^\alpha} = \frac{1}{2}\nabla^2 u(x,y,t) + u^2(1-u) + f(x,y,t), \tag{3.40}$$

where $f(x,y,t) = e^{xy}(1.91116t^{1.1} + e^{xy}t^4(-1 + e^{xy}t^2) - 0.5t^2(x^2+t^2))$ with the following initial and boundary conditions as

$$\begin{aligned} u(x,y,0) &= 0, \\ u(0,y,t) &= t^2, \\ u(x,0,t) &= t^2, \\ u(1,y,t) &= e^y t^2, \\ u(x,1,t) &= e^x t^2. \end{aligned} \tag{3.41}$$

The exact solution of this time-fractional Fisher's equation is $u(x,y,t) = e^{xy}t^2$ for the fractional order time parameter $\alpha = 0.9$. The absolute errors, order of convergence and the CPU time required for the PDE with the proposed method are given in Table 3.3 and Table 3.4 for $y = 0.5, 0 \le x \le 1$ and $x = 0.5, 0 \le y \le 1$, respectively for the order of approximation $N = 3, 5, 7$ at $t = 1$. The tables clearly exhibit that the proposed scheme is computationally effective even for less CPU time.

TABLE 3.3: Efficiency of the numerical method for Example 2 at $y = t = 0.5$

y	N	Maximal absolute error $0 \leq x \leq 1$	Order of convergence	CPU Time (second)
0.5	5	0.00026	-	7.12
	7	0.000041	5.48	9.36
	9	0.0000067	7.20	10.55

TABLE 3.4: Efficiency of the numerical method for Example 2 at $x = t = 0.5$

x	N	Maximal absolute error $0 \leq y \leq 1$	Order of convergence	CPU Time (second)
0.5	5	0.0003	-	7.10
	7	0.000039	6.06	9.41
	9	0.0000064	7.19	10.48

The absolute error between the numerical solution and the exact solution is depicted through Fig. 3.3 at $t = 1$ for various values of x and y.

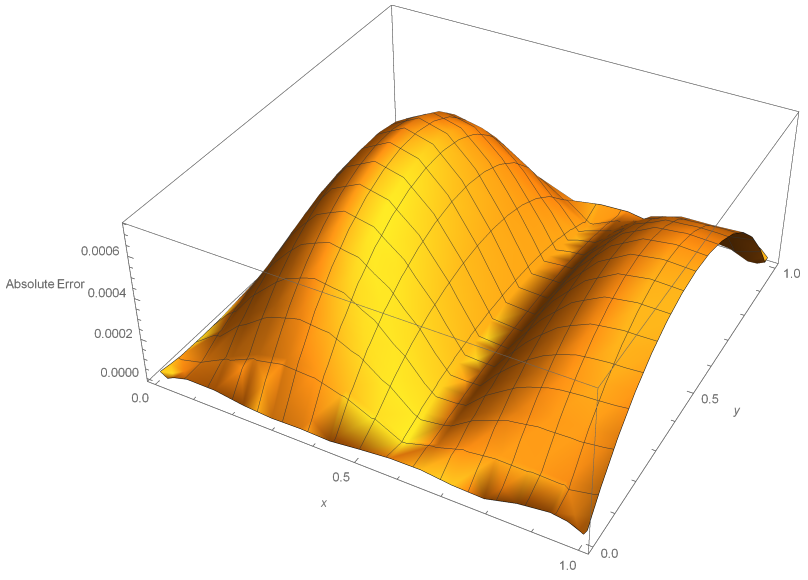

FIGURE 3.3: Plot of the absolute error between the exact and numerical solutions vs. x and y at $t = 1$.

Fig. 3.3 shows that the numerical solution is approximately accurate to the exact solution even for $N = 5$. The better convergence can be achieved with the increase in N.

Example 3. Consider following two-dimensional non-linear non-homogeneous fractional order reaction-advection-diffusion equation as

$$\frac{\partial^\alpha u}{\partial t^\alpha} = \frac{\partial^2 u}{\partial x^2} + \frac{\partial^2 u}{\partial y^2} + \frac{\partial u}{\partial x} + \frac{\partial u}{\partial y} + u(1-u) + f(x,y,t), \tag{3.42}$$

where $f(x,y,t) = 1.91116t^{1.1}x^2y^2 + t^4x^4y^4 + t^2(-2xy^2 - 2y^2 + x^2(-2-y^2)) - 2x^2yt^2$ with the following initial and boundary conditions

$$\begin{aligned} &u(x,y,0) = 0,\\ &u(0,y,t) = 0,\\ &u(x,0,t) = 0,\\ &u(1,y,t) = y^2t^2,\\ &u(x,1,t) = x^2t^2. \end{aligned} \tag{3.43}$$

The exact solution for this concerned example is $u(x,y,t) = x^2y^2t^2$ for fractional order time parameter $\alpha = 0.9$. The absolute errors, order of convergence and the CPU time required for the PDE with the proposed method are given in Table 3.5 and Table 3.6 for $y = 0.5, 0 \le x \le 1$ and $x = 0.5, 0 \le y \le 1$, respectively for the order of approximation $N = 5, 7, 9$ at $t = 1$. It is clear from the tables that the proposed scheme is computationally effective even for less CPU time.

TABLE 3.5: Efficiency of the numerical method for Example 3 at $y = t = 0.5$

y	N	Maximal absolute error $0 \le x \le 1$	Order of convergence	CPU TIME (second)
0.5	5	0.00033	-	7.47
	7	0.000028	7.33	10.54
	9	0.0000022	10.12	12.35

TABLE 3.6: Efficiency of the numerical method for Example 3 at $x = t = 0.5$

x	N	Maximal absolute error $0 \le y \le 1$	Order of convergence	CPU Time (second)
0.5	5	0.00038	-	7.47
	7	0.000032	7.35	10.53
	9	0.0000026	9.98	12.35

The absolute error between the numerical solution and the exact solution is depicted through Fig. 3.4 at $t = 1$ for various values of x and y.

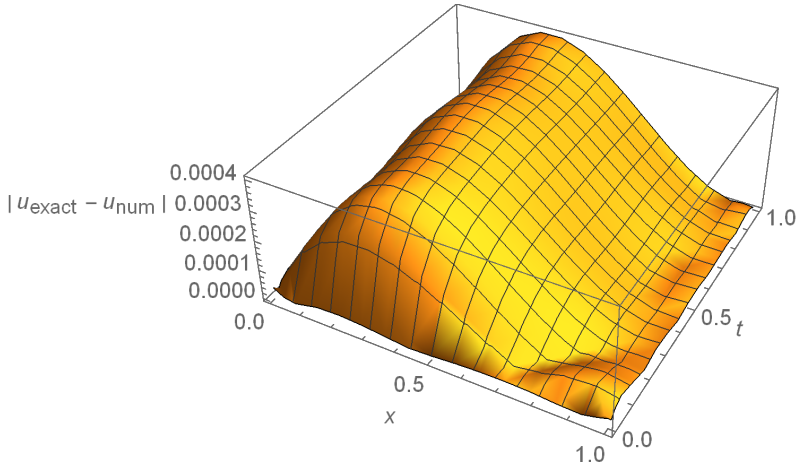

FIGURE 3.4: Plot of the absolute error between the exact and numerical solutions vs. x and t at $y = 0.5$.

Fig. 3.4 shows that the numerical solution is approximately accurate to the exact solution even for $N = 5$. The better convergence can be achieved with increase in N.

3.8 Results and discussion for proposed model

After being a justification of the accuracy and effectiveness of the method, the author has been motivated to apply his proposed numerical scheme to solve the concerned two-dimensional nonlinear time fractional order reaction-diffusion model (3.4) under the prescribed initial and boundary conditions (3.5). The variations of the solute concentration $u(x, y, t)$ vs. the column lengths x and y at $t = 0.5$ for various values of the fractional order time parameter α for conservative case ($k = 0$) and non-conservative case ($k \neq 0$) are calculated numerically and are displayed graphically through Figs. 3.5-3.7.

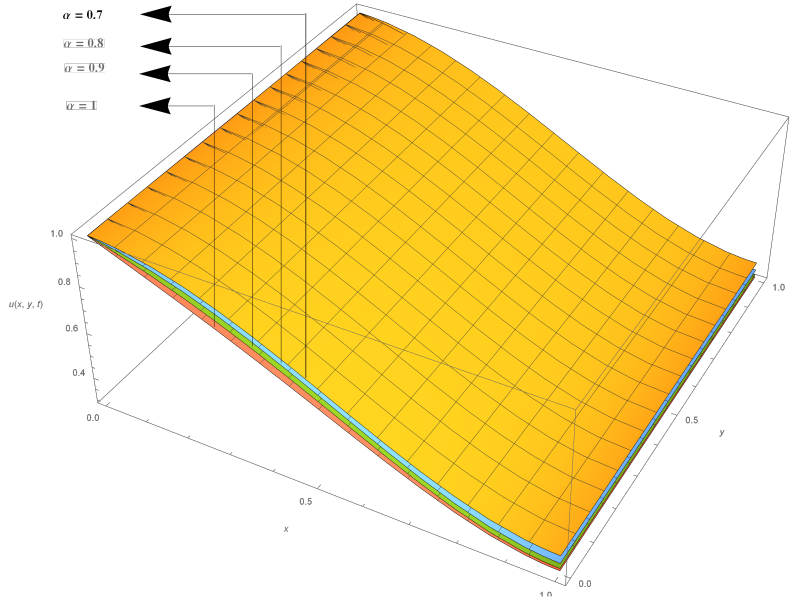

FIGURE 3.5: Plots of the field variable $u(x, y, t)$ vs. x and y at $t = 0.5$ for $k = -1$ for different values of α.

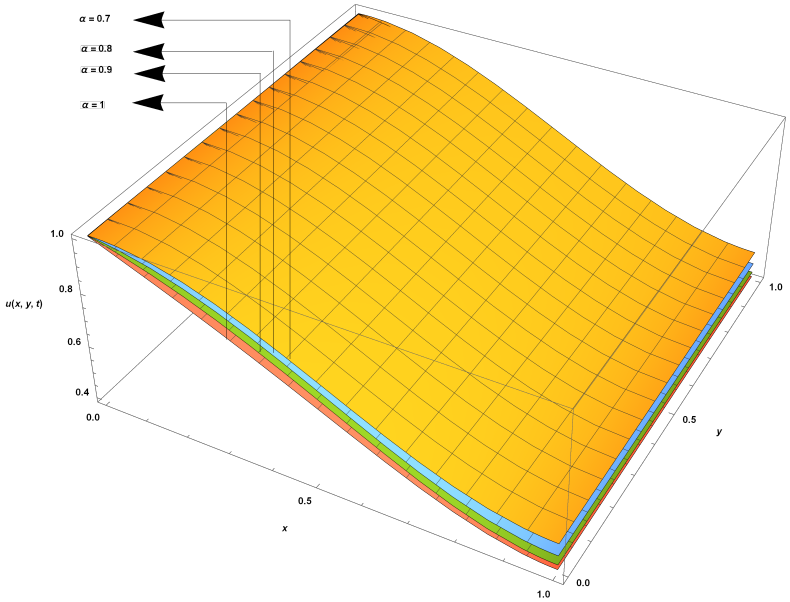

FIGURE 3.6: Plots of the field variable $u(x, y, t)$ vs. x and y at $t = 0.5$ for $k = 0$ for different values of α.

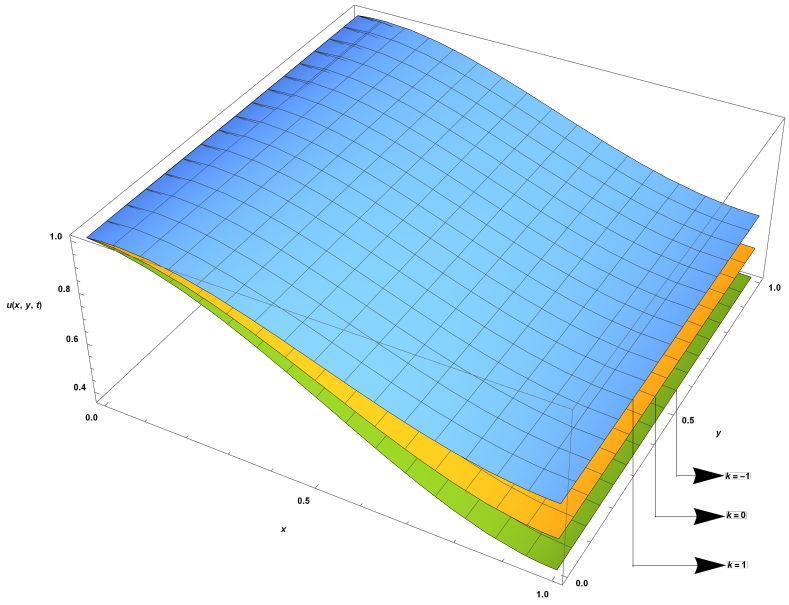

FIGURE 3.7: Plots of field variable $u(x, y, t)$ vs. x and y at $t = 0.5$ for $\alpha = 0.7$ for different values of k.

The effects of reaction term on the solution profile for various values of the fractional order time derivative are found for $k = -1$ and $k = 0$, which are shown through Fig. 3.5 and Fig. 3.6, respectively. It is seen that the overshoots of sub-diffusion are decreased as the system advances towards fractional order from standard order. It is also seen from the figures that dampings are found due the presence of sink term ($k = -1$). Fig. 3.7 reveals that it consumes less time to stabilize the probability density function $u(x, y, t)$ at $t = 0.5$ for the case $\alpha = 0.7$ due to the effect of sink term $k = -1$ as compared to the case of $k = 0$ and also the presence of source term $k = 1$, which clearly shows that physical importance of the presence of sink term in the system to enhance the stability region.

3.9 Conclusions

Four objectives have been accomplished through the present scientific contribution. First one is finding the solute concentration $u(x, y, t)$ for two-dimensional non-linear fractional order reaction-diffusion equation employing the powerful and efficient technique Laguerre operational matrix. Second one is the pictorial presentations of the nature of overshoots in the form of sub-diffusion due to presence of reaction terms for different particular cases. The third one is the graphical presentations of the damping nature of the solute concentration when the system advances towards fractional order from standard order in

the presence of sink term. The most important part of the present study is the exhibition of the order of convergence during the validation of the proposed method while applying on the existing problems having analytical solutions.